

# REGULARITIES OF LIGHT DIFFUSION IN THE COMPOSITE MATERIAL PENTAERYTHRIOL TETRANITRATE – NICKEL

A. A. Zvekov<sup>1</sup>, M. V. Ananyeva<sup>2</sup>, A. V. Kalenskii<sup>2</sup>, A. P. Nikitin<sup>1</sup>

<sup>1</sup> Institute of Coal Chemistry and Material Science SB RAS, Kemerovo, Russia,

<sup>2</sup>Kemerovo State University, Kemerovo, Russia

kriger@kemsu.ru, zvekova@gmail.com

**PACS 52.25.Tx, 82.40.Fp**

The solution of the radiative transfer equation in the layer of a diffusing medium with Frenel fronts was observed by the example of light transfer in a dielectric medium containing nickel nanoparticles. The method of spherical harmonics was used. A scattering indicatrix was calculated for 532 nm light for 140 nm nickel nanoparticles in a pentaerythriol tetranitrate matrix. The angular distribution of illumination on the sample's fronts was calculated for reflected and transmitted light. The maximum of the scattering indicatrix is observed for the diffusion in the opposite direction. The minimum of the illumination on the front in direction of the sample's bulk is a result of using the Frenel's boundary conditions and the asymmetric property of the scattering indicatrix of the nickel nanoparticles. The possibility of using of the composites explosives – nickel nanoparticles as a cap of the optical detonator is considered.

**Keywords:** metal nanoparticles, simulation, diffusion of light.

*Received: 15 September 2014*

## 1. Introduction

Nanosystems based on transparent dielectrics containing light-absorbing and light-diffusing metal particles have wide practical application [1–7]. That is why the optical properties of metal nanoparticles in transparent media were studied in many experimental and theoretical works [8–12]. The applied side of the problem deals with the potential practical use light absorption and diffusion by nanoparticles in the semi-conductor solar battery [1]; in process of atmospheric sounding [2]; in analysis of biological [3] and alimentary [4] products; in the caps of optical detonators [5–7]. The complexity of the problem is caused by simultaneous absorption [8–13] and diffusion [8]. Using typical conditions for the experimental samples width and nanoparticle concentration [14], the multiple diffusion of light becomes more significant. This effect is described by the radiative transfer equation. To solve this type of problem, the diffusion approximation [15], Kubelka-Munk theory [9] and solution using Monte Carlo method [10] are typically applied. The reason for their popularity is the relative simplicity (diffusion approximation and Kubelka-Munk theory), and the availability of the ready code for process simulation (Monte Carlo method). At the same time, diffusion approximation and Kubelka-Munk theory might be used only in the extreme case of the very strong light diffusion [9] and for them, only approximate boundary conditions might be done. As a result, the application of these methods can cause some significant errors [9]. In most works on the radiative transfer, Marshal's boundary conditions are used [16]. Marshal's boundary conditions might be used as approximate conditions for the fronts on which the refractive index does not change. In case

of the systems where the refractive index does change on the fronts (for example, pressed nanocomposites dielectric-metal), it is necessary to use the Frenel's conditions [8]. In work [8], the adopted method of the spherical harmonics was proposed for use in cases of homogeneous layer radiative transfer. The aim of this work is the simulation of the diffusion of light by metal nanoparticle in transparent media in terms of radiative transfer theory by the example of pentaerythriol tetranitrate (PETN) containing nickel nanoparticles with defined sizes (average radius 140 nm).

## 2. Model

PETN samples containing nickel nanoparticles were chosen as a model system. The wavelength was 532 nm, which corresponds to the second harmonic of Nd:Yag laser. The model was chosen because of several advantages – this composite might be used as a cup of the optical detonators [7, 11, 12, 17, 18]; matrix material (PETN) might be pressed in order to get dense and optically transparent sample without visible imperfections; methods of synthesis of spherical nickel nanoparticles with necessary sizes are well known [19].

In terms of the radiative transfer theory, the matrix is characterized by the linear extinction coefficient  $k$ , the absorptivity  $k_{abs}$  and the scattering coefficient  $k_{sca}$ , the albedo of single interaction of the light quantum with the scattering media  $\Lambda = k_{sca}/k$  and the scattering indicatrix. Equations for the absorptivity, scattering coefficient, and extinction coefficient are the following [19]:

$$k_{abs} = \pi r_{eff}^2 Q_{abs} C, \quad k_{sca} = \pi r_{eff}^2 Q_{sca} C, \quad k = \pi r_{eff}^2 C \cdot (Q_{sca} + Q_{abs}), \quad (1)$$

where  $r_{eff}$  – inclusion's effective radius,  $C$  – inclusion's concentration ( $\text{cm}^{-3}$ ),  $Q_{abs}$  and  $Q_{sca}$  – the average values of the absorptivity and scattering coefficient of the nanoparticles. Effective radius was taken as 140 nm. Concentration was calculated using mass fraction. To solve the radiative transfer equation, a sort of spherical harmonics method was used, which divides the total illumination into the incident (nonscattered  $I_0$ ) and the scattered ( $I_s$ ), both giving ( $I = I_0 + I_s$ ). The nonscattered part decreases according to Bouguer's law taking into account back edge reflection. The differential equation system for the expansion coefficients of the reflected part of the illumination on the spherical harmonics ( $C_m$ ) is:

$$\begin{aligned} \frac{1}{2m+1} \cdot \left[ (m+1) \frac{dC_{m+1}}{d\tau} + m \frac{dC_{m-1}}{d\tau} \right] + \left( 1 - \frac{\Lambda x_m}{2} \right) C_m = \\ = \frac{J \Lambda x_l}{2} [\exp(-\tau) + R_f \exp(\tau - 2L)] \end{aligned} \quad (2)$$

where  $x_l$  – expansion coefficients of the scattering indicatrix on the spherical harmonics. Boundary conditions for (2) correspond to the Frenel's reflection:

$$I_s(0, \mu) = R(\mu) I_s(0, -\mu), \quad 0 \leq \mu \leq 1, \quad (3)$$

$$I_s(L, -\mu) = R(\mu) I_s(L, \mu), \quad -1 \leq \mu \leq 0, \quad (4)$$

where  $R(\mu)$  – angle dependence of the Frenel's reflection coefficient,  $\mu = \cos \theta$  – cosine of a spherical angle. Equations (3) – (4) define the boundary conditions on the top face and the back edge correspondingly. Expansion of  $R(\mu)$  in terms of Legendre polynomial gives the boundary condition for the harmonics' contributions:

$$\sum_{m=0}^N (N_{lm} - R'_{lm}) C_m(0) = 0, \tag{5}$$

where the matrix elements are the following:

$$\begin{aligned} R'_{lm} &= (-1)^m \frac{2m+1}{2} \int_0^1 P_m(\mu) R(\mu) P_l(\mu) d\mu, \\ N_{lm} &= \frac{2m+1}{2} \int_0^1 P_m(\mu) P_l(\mu) d\mu. \end{aligned} \tag{6}$$

Similar boundary conditions were made for the top face and the back edge of the sample. According to Frenel's equations, the angle dependence of the reflection coefficient while  $\mu \geq \sqrt{1 - n^{-2}}$  is the following:

$$R(\mu) = \frac{1}{2} \left( \frac{\sqrt{n^{-2} - 1 + \mu^2} - \mu}{\sqrt{n^{-2} - 1 + \mu^2} + \mu} \right)^2 \left[ 1 + \left( \frac{\mu \sqrt{n^{-2} - 1 + \mu^2} + \mu^2 - 1}{\mu \sqrt{n^{-2} - 1 + \mu^2} - \mu^2 + 1} \right)^2 \right]. \tag{7}$$

When  $\mu < \sqrt{1 - n^{-2}}$ , total reflection take place and  $R(\mu)=1$ .

For simulation, the first 20 harmonics ( $N = 19$ ) were used, because the further increase of their quantity does not change the calculation results. At the same time, using fewer components is not desirable because of the strong instability of the angle distribution.

Solution of (2) might be expressed as:

$$C_m(\tau) = \sum_{l=0}^N a_{ml} \tilde{C}_l \exp(\gamma_l \tau) + C_p^1 \exp(-\tau) + C_p^2 \exp(\tau). \tag{8}$$

The last two components are the particular solution for the heterogeneous equation. Coefficients  $C_p^1$  and  $C_p^2$  are equal to each other:

$$\begin{aligned} C_p^1 &= -J\Lambda \cdot \sum_{m=0}^N [\delta_{pm} + A_{pm}]^{-1} B_m, \\ C_p^2 &= J\Lambda R_f \exp(-2L) \cdot \sum_{m=0}^N [\delta_{pm} - A_{pm}]^{-1} B_m, \end{aligned} \tag{9}$$

where

$$\begin{aligned} A_{pm} &= - \left[ \frac{p+1}{2p+1} \delta_{p,p'+1} + \frac{p}{2p+1} \delta_{p,p'-1} \right]^{-1} \left[ \left( 1 - \frac{\Lambda x_m}{2} \right) \delta_{p'm} \right], \\ B_m &= \left[ \frac{m+1}{2m+1} \delta_{m,m'+1} + \frac{m}{2m+1} \delta_{m,m'-1} \right]^{-1} \left[ \frac{x_{m'}}{2} \right]. \end{aligned}$$

Two multipliers in square brackets are multiplied as matrixes. The first component in (8) corresponds to the expansion of the solution on the eigenvector of  $A_{pm}$  (matrix  $a_{ml}$ ) according to the corresponding eigenvalue  $\gamma_l$ . Expansion coefficients  $\tilde{C}_l$  must be defined in the form of the boundary conditions (3) – (4). These boundary conditions make system of  $2N + 2$  equations,  $2N$  of which are linearly dependent. Number of coefficients which might be defined is  $N + 1$ , so that the problem is overspecified. So it was decided to use the minimizing of sum of deviation squares of the values in the left parts (3) – (4) from zero. As a result, the following equation (in matrix form) for the coefficients was obtained:

$$\tilde{C} = - \left[ (Z\tilde{a})^T (Z\tilde{a}) \right]^{-1} (Z\tilde{a})^T (ZC_p), \quad (10)$$

where

$$Z = \begin{pmatrix} N - R' \\ \tilde{N} - \tilde{R}' \end{pmatrix}, \quad \tilde{a} = \begin{pmatrix} a \\ a \cdot \exp(-\gamma L) \end{pmatrix}, \quad C_p = \begin{pmatrix} C_p^1 \\ C_p^2 \end{pmatrix}.$$

### 3. Results and discussion

In figure 1, the scattering indicatrix, calculated in terms of Mie theory, of the 140 nm nickel nanoparticles in PETN matrix for the second harmonic of Nd:Yag laser is presented. The maximum of the scattering indicatrix corresponds to the point  $\mu = -1$ . This means that the light mainly reflects in the opposite direction of the incident light. The indicatrix shape is defined by the relatively large particles' radii when the modulus of the nickel's complex refractive index is significant ( $1.87 - 3.49i$ ). The anisotropy factor (the average value of the scattering angle cosine) is  $-0.833$ . As it stands, the calculated values for the scattering coefficient  $Q_{sca}$  and absorptivity  $Q_{abs}$  for the nickel nanoparticles are 2.109 and 1.199 respectively. The efficiencies of both these processes are high because the irradiation wavelength in the medium is comparable to the nanoparticles' diameters.

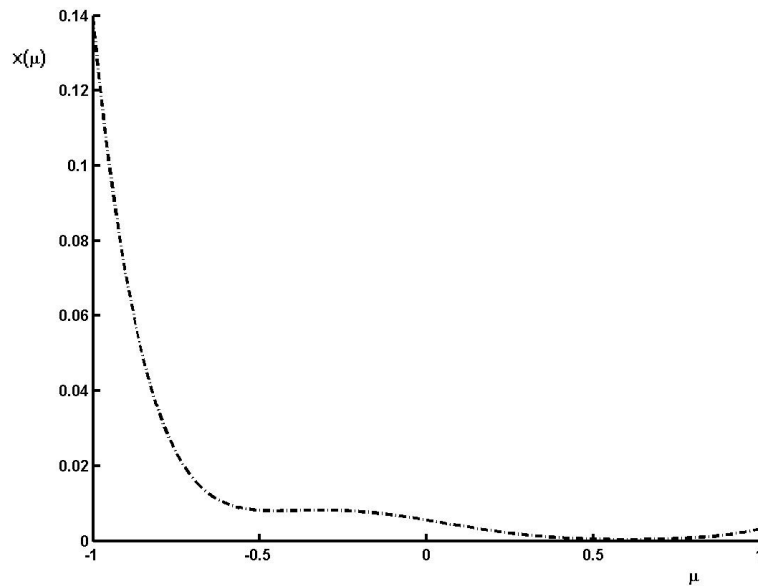


FIG. 1. Scattering indicatrix of the nickel nanoparticles in PETN matrix for 532 nm wavelength

Figure 2 shows distribution of the absorbed energy along the sample (1). Contributions of the nonscattered (2) and scattered part (3) are separately matched. The nonscattered part refers to the irradiation which is absorbed directly by the sample at first interaction. This part decreases according to the Bouguer law with the coefficient which is equal to the ratio of extinction. Scattered part includes all the radiation, which was at least once scattered. This part was calculated using equation (2). The scattered part decreases more slowly in the sample bulk and near to the top face, having a slanting maximum, concerning the partial permittivity of the border to the irradiation. Total dependence (1) is close to the exponential dependence with some deviations in the vicinity of the sample's borders. At some distance away from the border the dependence is close to the exponential with absorptivity equal to  $\kappa = 26.74 \text{ cm}^{-1}$ .

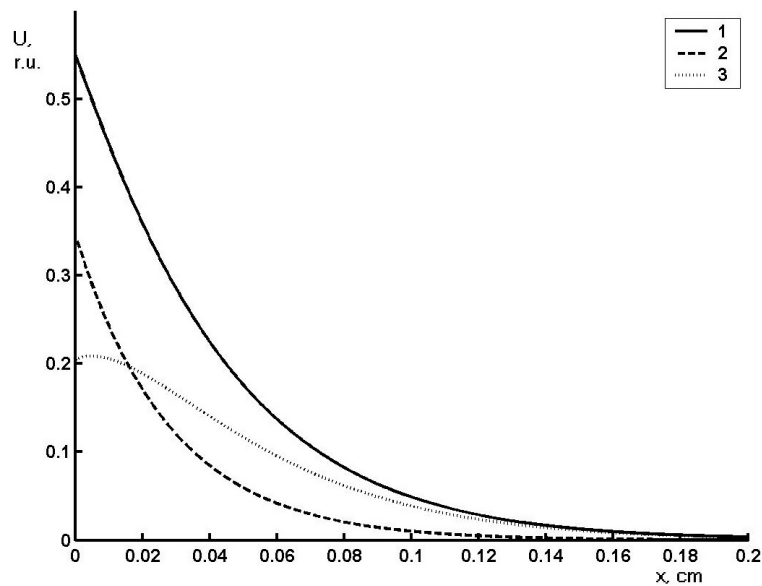


FIG. 2. Distribution of absorbed energy of irradiation (1) along the composite PETN – nickel with the nickel's mass fraction 0.1%, contributions of the non-scattered (2) and scattered part (3)

Figure 3 shows the results of simulation of the angle dependence the scattered and transmitted irradiation (relative units) for the samples where the nickel's mass fraction equal to 0.1% (nanoparticle's radius is 140 nm). The sample width is 0.1 cm, which is almost four times the extinction length. For wider samples, the transmission coefficient becomes a negligible quantity. Values of the transmission and reflection coefficients are 0.060 and 0.169 correspondingly. Let us now discuss the main particularities of the obtained angle dependences. In the case of reflected light, the distribution of intensity has two local minima in the vicinity of  $\mu \approx 0.9$  (moving into the sample, perpendicularly to the top face) and two slanting maxima in the vicinity of  $\mu \approx -0.5$  and  $\mu \approx 0.5$ . At the point  $\mu = -1$ , there is a maximum for the reflected light intensity, so the reflected light is mostly reflected in the opposite direction. In case of transmitted light, there is the opposite situation – the maximum of light intensity is in the area of the reflected light minimum, i.e. near  $\mu = 1$ . The minimum of the calculated dependences in the area of the normal direction of light into the sample is explained by the use of Frenel's boundary conditions (3) – (4). The maxima appear because the scattering indicatrix of the nickel nanoparticles is very dissymmetric (Fig. 1).

Let us estimate the extension factor of absorption in the conditions of multiple scattering. The extension factor might be determined as ratio of the absorption cross-section, calculated using the absorptivity, and the nanoparticle's geometric cross-section –  $K = \kappa / (\pi r_{eff}^2 C)$ . Substitution gives the following value  $K = 2.51$ . It is necessary to mention that this value is greater than 1 not only because of the large absorptivity ( $Q_{abs} = 1.199$ ), but mainly because of multiple scattering.

The results are very important in order to determine the cap composition for optical detonators. Nickel nanoparticles with an average size of 140 nm might be a very promising additive in the transparent explosives (particularly in PETN, initiated by the second harmonic of the Nd:Yag laser), i.e. because of the multiple scattering and large absorptivity value, light absorption is considerably amplified. This must cause corresponding decrease of the critical energy density of the laser initiation.

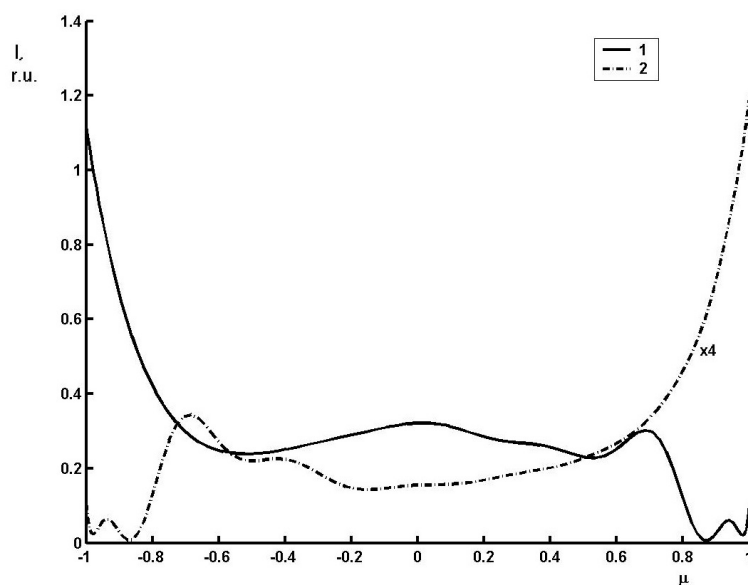


FIG. 3. Angle distribution of the scattering part of illumination on the sample's borders by the reflected (1) and transmitted (2) light

### Acknowledgments

This work was supported by Ministry of Education and Science of the Russian Federation (governmental project No. 2014/64) and Russian Foundation for Basic Research for the financial support (grant No. 14-03-00534 A).

### References

- [1] Moulin E., Sukmanowski J., et al. Improved light absorption in thin-film silicon solar cells by integration of silver nanoparticles. *Journal of Non-Crystalline Solids*, **354**, P. 2488–2491 (2008).
- [2] Kochikov I.V., Morozov A.N., Fufurin I.L. Numerical procedures for substances identification and concentration calculation in the open atmosphere by processing a single FTIR measurement. *Computer Optics*, **36** (4), P. 554–561 (2012).
- [3] Lisenko S.A., Kugeiko M.M., Firago V.A., Sobchuk A.N. Noninvasive express analysis of hemoglobin derivatives in blood by reflectance spectroscopy. *Journal of Applied Spectroscopy*, **81** (1), P. 120–128 (2014).
- [4] Rey J.M., Kottman J., Sirgist M.W. Photothermal diffuse reflectance: a new tool for spectroscopic investigation in scattering solids. *Applied Physics B*, **112** (4), P. 547–551 (2013).
- [5] Kriger V.G., Kalenskii A.V., et al. Heat transfer processes during laser heating included in an inert matrix. *Teplofizika and aeromekhanika*, **20** (3), P. 375–382 (2013).
- [6] Chumakov Yu.A., Knyazeva A.G. Initiation of reaction in the vicinity of a single particle heated by microwave radiation. *Fizika gorennya i vzryva*, **48** (2), P. 24–30 (2012).
- [7] Ananyeva M.V., Zvekov A.A., et al. Promising compounds for the cap of optical detonator. *Perspektivnye materialy*, **7**, P. 5–12 (2014).
- [8] Aduv B.P., Nurmukhametov D.R., et al. Integrating Sphere Study of the Optical Properties of Aluminum Nanoparticles in Tetrantropentaerytrite. *Zhurnal Tekhnicheskoi Fiziki*, **84** (9), P. 126–131 (2014).
- [9] Sandoval C., Kim A.D. Deriving Kubelka-Munk theory from radiative transport. *Journal of Optical Society of America A*, **31** (3), P. 628–636 (2014).
- [10] Hayakawa C.K., Spanier J., Venugopalan V. Comparative analysis of discrete and continuous absorption weighting estimators used in Monte Carlo simulations of radiative transport in turbid media. *Journal of Optical Society of America A*, **31** (2), P. 301–311 (2014).
- [11] Kriger V.G., Kalenskii A.V., et al. Influence the efficiency of absorption of the laser radiation on the temperature of the heating inclusion in transparent glass. *Fizika gorennya i vzryva*, **48** (6), P. 54–58 (2012).
- [12] Zykov I.Y. Accounting of the absorbance of nano-inclusions heated by laser impulse. *Mezhdunarodnoe nauchnoe izdanie 'Sovremennyye fundamentalnyie i prikladnyie issledovaniya'*, **3** (6), P. 42–48 (2012).

- [13] Aduiev B.P., Nurmukhametov D.R., et al. Explosive decomposition of TEN with nanoadditives aluminum under the action of pulsed laser radiation of different wavelengths. *Khimicheskaya fizika*, **32** (8), P. 39–42 (2013).
- [14] Kalenskii A.V., Zvekov A.A., et al. Influence of the laser irradiation wavelength on the energetic materials' initiation critical energy. *Fizika gorennya i vzryva*, **50** (3), P. 98–104 (2014).
- [15] Gao M., Huang X., Yang P., Kattawar G.W. Angular distribution of diffuse reflectance from incoherent multiple scattering in turbid media. *Applied Optics*, **52** (24), P. 5869–5879 (2013).
- [16] Budak V.P. *Methods of solution the radiative transfer equation*. Publishing house MEI, Moscow, 52 p. (2007).
- [17] Ananyeva M.V., Kalenskii A.V., et al. Kinetic regularities of the explosive decomposition of PETN containing nanosized inclusions of aluminium, cobalt, and nickel. *Bulletin of Kemerovo State University*, **1-1** (57), P. 194–200 (2014).
- [18] Kalenskii A.V., Ananyeva M.V., Zvekov A.A., Zikov I.Yu. Spectrum dependence of the critical energy density of composites based on pentaerythritol tetranitrate with nikel nanoparticles. *Fundamental'nye problemy sovremennogo materialovedeniya*, **11** (3), P. 340–345 (2014).
- [19] Zakharov Y.A., Pugachev V.M., et al. Structure of nanosize bimetal Fe–Co and Fe–Ni. *Bulletin of the Russian Academy of Sciences: Physics*, **77** (2), P. 142–145 (2013).